THE JOURNAL OF PHYSICAL CHEMISTRY C

Article

pubs.acs.org/JPCC

First-Principles Study of the Nuclear Dynamics of Doped Conjugated Polymers

Jun Yin,[†] Zilong Wang,[†] Daniele Fazzi,*[,‡] Zexiang Shen,[†] and Cesare Soci*[,†]

[†]Division of Physics and Applied Physics, School of Physical and Mathematical Sciences, Nanyang Technological University, 21 Nanyang Link, Singapore 637371

[‡]Max-Planck-Institut für Kohlenforschung (MPI-KOFO), Kaiser-Wilhelm-Platz 1, D-45470 Mülheim an der Ruhr, Germany

Supporting Information

ABSTRACT: Infrared-active vibrational (IRAV) modes are specific optical fingerprints to probe the density, dynamics, and spatial distribution of polarons in π-electron conjugated polymers. So far, the description of IRAV mode activation and selection rules, resulting from the local breaking of spatial symmetry induced by charge carriers, has been restricted to phenomenological lattice-dynamics models. Overcoming the classical picture, here we combine first-principles calculations with vibrational spectroscopy to study the nuclear dynamics of a model polymer system, poly(3-hexylthiophene) (P3HT). We assign and reproduce quantitatively the transition energies and intensities of vibrational normal modes in the ground and excited electronic states. By comparing the ground, polaronic, and excitonic states of regioregular (RR-) and regiorandom (RRa-) chains, we identify, for the first time, the vibrational fingerprints of neutral singlet excitations in the IRAV spectra of P3HT and highlight structure−property correlations. Within this new approach, vibrational spectroscopy provides a comprehensive tool to study not only polaron but also exciton density and dynamics and to better understand the influence of disorder on exciton and charge-carrier localization in functional organic systems.

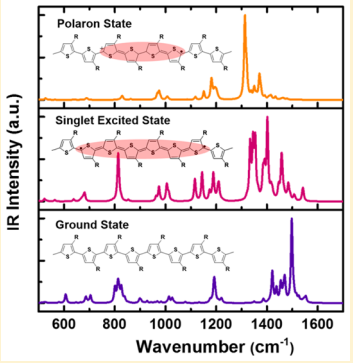

A thorough understanding of the relationship between molecular structure and optoelectronic properties is essential to design organic functional materials and optimize their device performance.[1−5] Key structural characteristics, such as molecular order, bonds pattern, and spatial extent of charged and excited states, are intimately related to the free carrier mobility and exciton lifetime, which ultimately determine the efficiency of organic devices, such as polymer field effect transistors and solar cells. Because of the large electron−phonon coupling, changes in the electronic structure of π-conjugated polymers lead to significant variations in the nuclear structure and dynamics.[6−11] Thus, vibrational (IR and Raman) spectroscopy, which is sensitive to variations of local dipole moments and polarizability within the nuclear oscillations, has been the technique of choice to understand electronic and nuclear structures, charge generation, and charge/energy transfer mechanisms in these systems.[12−16]

In π-electron conjugated polymers with symmetric structure, collective oscillations in which the bond length alternation varies in phase[6] are Raman-active normal modes (i.e., g-symmetric) but IR-silent.[17−19] These oscillations are particularly sensitive to the electronic structure and conjugation length of the systems: the higher the electron delocalization, the lower the energy of the vibrational transition associated with the collective oscillation and the higher the Raman intensity.[3,20] These Raman-active modes may be turned into infrared-active vibrational (IRAV) modes once charge carriers are injected onto the polymer chain and self-localize, breaking the local spatial symmetry of the backbone.[21,22]

IRAV modes are arguably the most specific optical probe for charged excitation density[23] and dynamics[24,25] in π-electron-conjugated polymers upon photo-, electro-, or chemical-induced doping.[26−28] After the first experimental observation of IR-active modes in chemically doped polyacetylene by Fincher and coworkers,[29] similar modes were also observed upon photoexcitation of polyacetylene and attributed to charged solitons.[30] In nondegenerate ground state polymers, IRAV modes are directly related to charged polarons.[23,31] Thanks to their specificity and sensitivity, over the past two decades IRAV modes have been largely employed as a direct probe of polaron density in pristine polymers,[26,28,32] charge-transfer processes and polaron dynamics in donor−acceptor blends,[23,31,33,34] structure−charge relationships in polymers,[26,35,36] polaron spatial distribution within the active region of working devices,[37,38] and, most recently, coupling of polarons to surface plasmons in infrared nanoantennas.[39]

From the theoretical standpoint, substantial work was done to understand and rationalize the description of IRAV modes. The first successful model capable of reproducing the key properties (frequency, relative intensities, and their one-to-one coincide with Raman modes) of the IRAV modes was

Received: December 1, 2015
Revised: January 4, 2016
Published: January 5, 2016

DOI: 10.1021/acs.jpcc.5b11764
J. Phys. Chem. C 2016, 120, 1994−2001

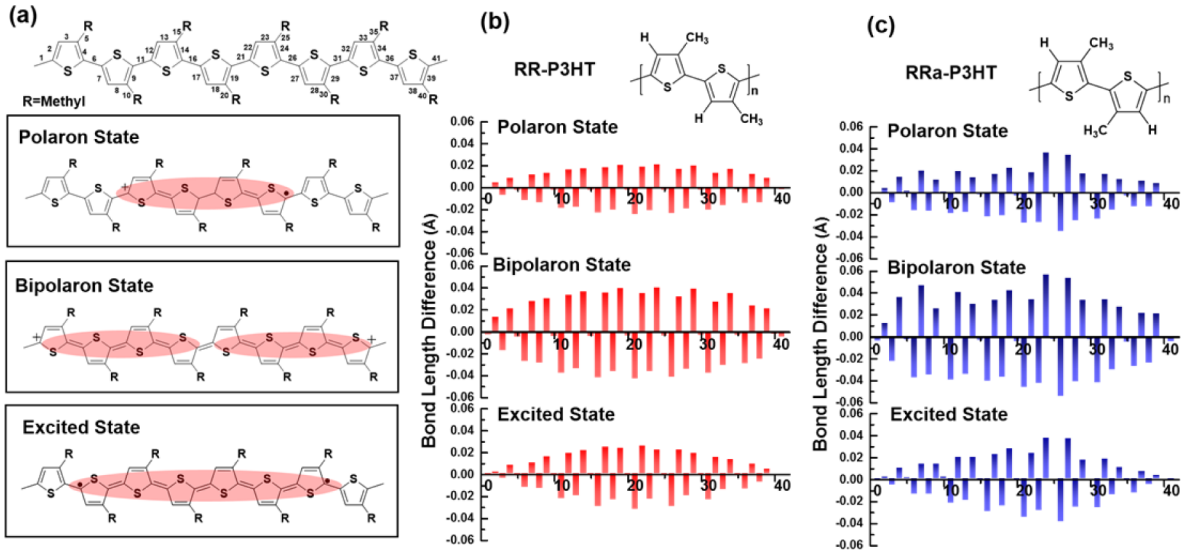

Figure 1. (a) Schematic molecular structures of ground, polaron, bipolaron, and excited state of RR-P3HT. (b,c) Bond length difference (BLD) for polaron, bipolaron, and excited state (i.e., S_1) RR- (b) and RRa- (c) oligomers, computed with respect to their ground-state structure.

developed by Horovitz et al. considering the pinning potential of the polymer skeleton chain.[40,41] Later on, Zerbi et al. developed a theory based on the effective conjugation coordinate (ECC) to explain and interpret the activation of IRAV modes and the phonon dispersion curves of π-electron conjugated systems.[42] IRAV spectral signatures have also been described within the framework of the amplitude mode model in Peierls organic semiconductors, and their lineshapes have been well reproduced by Fano-type antiresonances between the discrete IRAV modes and the low-energy broad polaron band.[32,43]

Despite the significant advances of these theoretical models for the IRAV modes in organic semiconductors, so far most descriptions have been based on phenomenological assumptions. To date, some fundamental aspects of vibrational modes in photo- or chemical-induced absorption spectra, such as their dependence on spatial delocalization of excited states and the quantitative assignment of vibrational modes to specific photoexcitations, remain unclear. Here we combine first-principles response calculations and infrared and Raman spectroscopy to study the vibrational properties of regioregular (RR-) and regiorandom (RRa-) poly(3-hexylthiophene) (P3HT), a model polymer system to understand the influence of structural order on photoconductive properties. By combining density functional theory (DFT) and time-dependent DFT (TD-DFT) calculations,[44,45] we reproduce and distinguish frequencies and relative intensities of ground, charged, and singlet excited-state vibrational normal modes and specifically assign their spectroscopic fingerprints. Besides *conventional* IRAV modes due to local symmetry breaking, we identify excitonic fingerprints in the photoexcitation spectrum due to the strengthening of specific bonds upon generation of singlet excitons. Furthermore, we relate the splitting of the C=C Raman and excited-state absorption bands and the C−S stretching peaks to the polymer regioregularity, providing a new indicator of the degree of structural order of polymeric chains.

DFT calculations were performed to study the geometries of neutral (P3HT), radical cation ($P3HT^{+}$, i.e., polaron), and radical dication ($P3HT^{+2}$, i.e., bipolaron) electronic states and corresponding vibrational modes by adopting restricted and unrestricted B3LYP functional, with 6-31G(d) basis set. The choice of a rather low basis set (i.e., the 6-31G(d)) was required for the evaluation of both equilibrium geometries and vibrational force fields of long oligomers (e.g., eight repeat units) in the ground, charged (+1 and +2), and excited electronic states. P3HT was represented by finite length oligomers (eight repeat units) to mimic the properties of the corresponding polymer;[46] side hexyl chains were replaced by methyl, and both RR- and RRa- substitutions were taken into account. The geometries and vibrational force fields of the lowest (dipole active) excited state (S_1, labeled as $^1P3HT^*$) were obtained through TDDFT calculations (TD-B3LYP/6-31G(d)) for both RR-P3HT and RRa-P3HT oligomers, without any symmetry constrain. All calculations were performed using the Gaussian09 program (revision D.01).[47]

Figure 1 shows the main skeletal molecular structures and bond length variations for RR-P3HT and RRa-P3HT evolving from the ground state to the (i) polaron, (ii) bipolaron, and (iii) first dipole allowed excited state (S_1). The structural variations induced by the different excitations i−iii are mainly localized in the central part of the chain and differ only in terms of *extension* and *amplitude* due to the different local molecular order and regioregularity of RR- versus RRa-P3HT. Polymer regioregularity affects the *amplitude* of the structural defects (e.g., bond lengths and torsional variations), with RRa-P3HT showing higher structural reorganizations than RR-P3HT, for each excitation. For the polaron (Figure 1b,c) the maximum bond length deformation (BLD) is ∼0.02 Å for RR- and ∼0.04 Å for RRa-P3HT, while for the bipolaron (Figure 1b,c) the structural changes are larger, with a maximum BLD of ∼0.04 Å for RR- and ∼0.06 Å for RRa-P3HT. The first excited-state equilibrium structure features a maximum BLD of ∼0.03 Å for RR- and ∼0.04 Å for RRa-P3HT. Different structural relaxations imply different electron−phonon coupling factors, which would, in turn, affect the vibrational properties (IR, Raman, and IRAV modes). Starting from a nonplanar ground state, with an average angle of ∼16° for RR- and ∼48° for RRa-P3HT, we find that all excitations (i−iii) induce a quinoidal-like, planar molecular structure in both RR and RRa cases (see Figure S1, Supporting Information).[48,49] The *defect extensions*

DOI: 10.1021/acs.jpcc.5b11764
J. Phys. Chem. C 2016, 120, 1994−2001

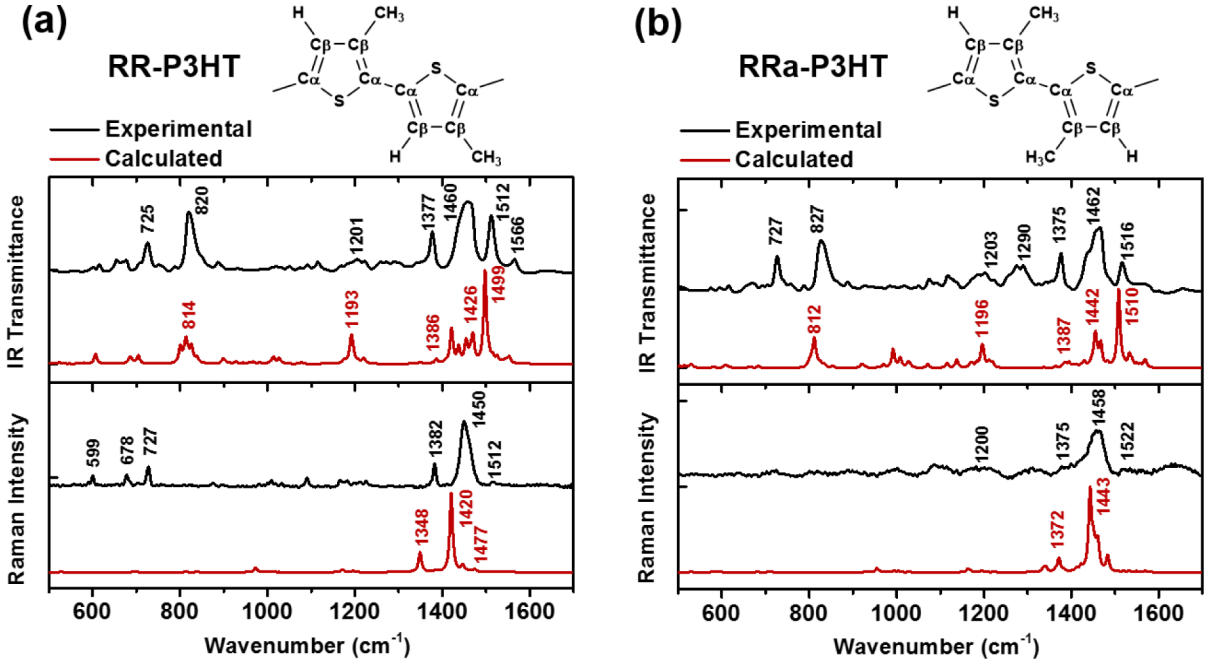

Figure 2. Experimental and calculated IR and Raman spectra of (a) RR- and (b) RRa-P3HT. The experimental IR and Raman spectra were measured in the thick film of RR- and RRa-P3HT on CaF_2 substrates.

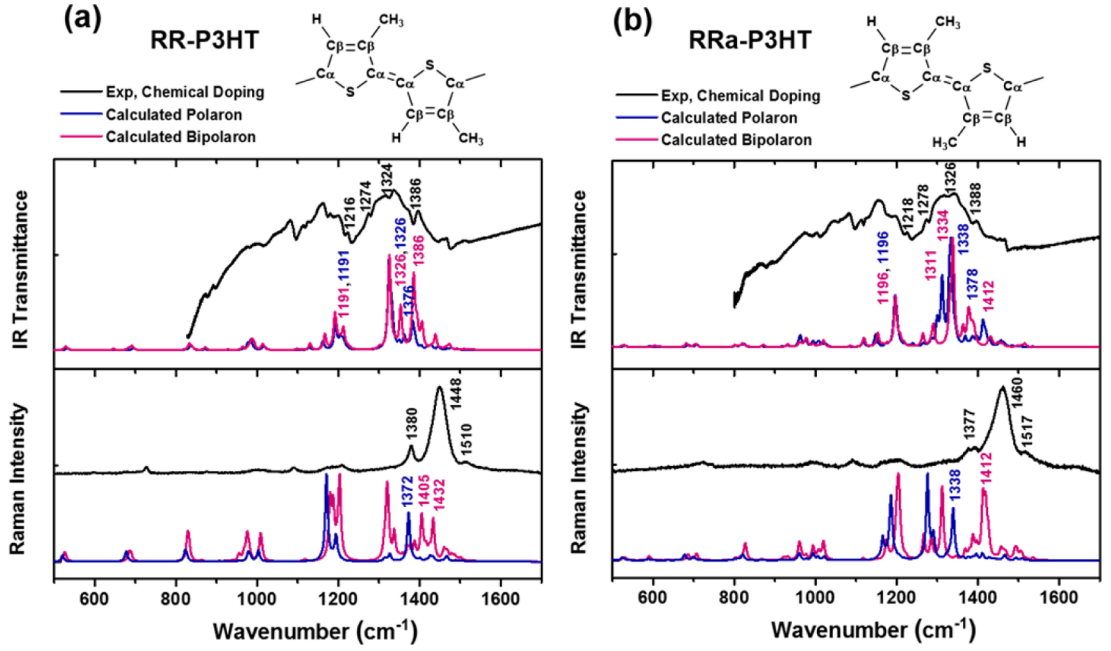

Figure 3. Experimental and calculated IR and Raman spectra of charge states of (a) RR-P3HT and (b) RRa-P3HT. The experimental IR and Raman spectra were measured in the thick film of $FeCl_3$-doping RR- and RRa-P3HT on CaF_2 substrates.

(i.e., the length for which BLDs are >0.015 Å) for polaron, bipolaron, and S_1 are 18.2, 28.8, and 14.3 Å for RR-P3HT and 19.6, 27.3, and 15.7 Å for RRa-P3HT. In both cases, the bipolaron results to be the most extended defect. Note that the computed defect amplitudes and extensions may be affected by the choice of the exchange-correlation DFT functional. B3LYP is known to overdelocalize the extension of the defect,[50,51] a tendency corrected by introducing range-separated functionals (e.g., CAM-B3LYP, ωB97XD, or BNL; see ref 52). Nevertheless, we decided to use this functional because of its documented reliability in predicting force constants and vibrational spectra for both neutral and charged/excited states.[53,54]

Figure 2 compares the experimental and calculated IR absorption spectrum of neutral RR- and RRa-P3HT in the range 500−1700 cm^{-1} (the frequency values associated with the main experimental IR and Raman peaks are also reported in the Figure; the corresponding eigenvectors can be found in Figures S4−S6 of Supporting Information). The calculated frequencies were scaled by the standard scaling factor of 0.9594 for the B3LYP functional to compare the DFT results with experimental spectra.[55]

DOI: 10.1021/acs.jpcc.5b11764
J. Phys. Chem. C 2016, 120, 1994−2001

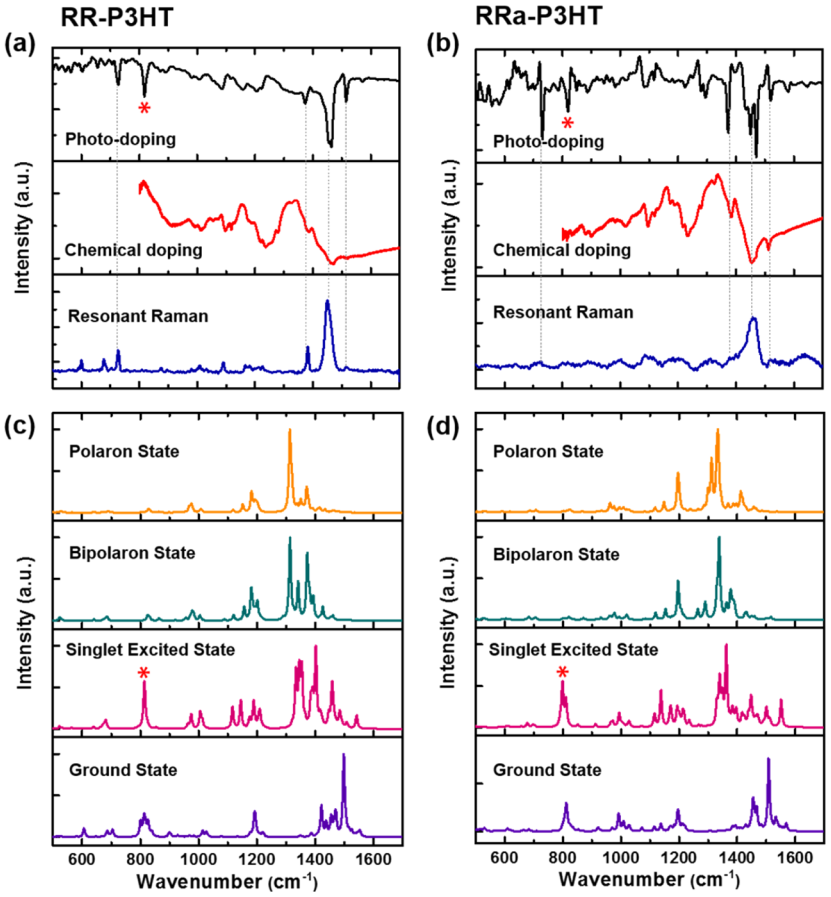

Figure 4. Photo and chemically induced absorption spectra of (a) RR- and (b) RRa-P3HT and the corresponding calculated IR spectra of polaron, bipolaron, excited (singlet), and ground states of (c) RR- and (d) RRa-P3HT. Vertical dashed lines indicate the conventional IRAV modes; the red asterisks show the newly identified excitonic mode.

The calculated IR spectrum of the neutral species reproduces well the main experimental features, similar to previous results for polythiophene[56] and derivatives.[57−59] In both RR- and RRa-P3HT, the most relevant backbone modes are the following:

(1) the 820 (RR-) and 827 (RRa-) cm^{-1} (calculated: 814 and 812 cm^{-1}) bands due to the C_β−H out-of plane deformations[56]

(2) the two bands in the 1420−1520 cm^{-1} spectral region due to the carbon−carbon bonds stretching vibrations of the thiophene rings.

The broad band around 1460 (RR-) and 1462 (RRa-) cm^{-1} (calculated: 1426 and 1442 cm^{-1}) is associated with symmetric C_α=C_β bonds stretching vibrations, while the peaks at 1512 (RR-) and 1516 (RRa-) cm^{-1} (calculated: 1499 and 1510 cm^{-1}) are related to antisymmetric C_α=C_β bonds stretching vibrations. Moreover, the vibrational fingerprints of hexyl side chains are observed at 725 and 1377 cm^{-1} for RR-P3HT, and 727 and 1375 cm^{-1} for RRa-P3HT, which can be assigned to the rocking vibration of methyl substituent and deformation of terminal methyl groups.

The simulations of Raman spectra are also in good agreement with experiments: when increasing the number of thiophene rings from 2 to 8, the computed spectrum red shifts (by ∼12 cm^{-1}) and the peak energies approach the experimental values (refer to Figure S3 in Supporting Information). Among the few Raman active modes in the 500−1700 cm^{-1} spectral region, the two in-plane ring skeleton modes at 1382 and 1450 cm^{-1} for RR-P3HT and 1375 and 1458 cm^{-1} for RRa-P3HT, due to the C−C and C=C stretching modes, are most sensitive to π-electron delocalization; the ratio of single to double carbon bond stretching mode intensity is a good indicator of the conjugation length ($I_{C-C}/I_{C=C}$):[57] here we obtain $I_{C-C}/I_{C=C}$ of 0.24 and 0.14 for RR- and RRa-P3HT, respectively. Noticeably, the computed peak at 1443 cm^{-1} splits into two peaks in the case of RRa-P3HT, as also reflected in photoinduced absorption spectra (see later discussion). The two peaks are assigned to symmetric C=C/C−C stretching/shrinking modes localized on different segments of the long oligomer chain.

After reproducing the vibrational properties of the polymers in the ground state, we calculated the vibrational properties of the polymers in the polaronic states. The results can be directly compared with the IR and Raman spectra of chemically doped polymers, where polarons and bipolarons are permanently induced. Figure 3 shows the experimental IR and Raman spectra of $FeCl_3$ doped RR- and RRa-P3HT, together with DFT calculated spectra for polarons and bipolarons. Because of the overlap between the broad polaron "P_0 band" and the sharp vibrational resonances,[32,43] the vibrational modes appear as Fano antiresonances (spectral dips) in the IR transmittance spectra of chemically doped P3HT. For both RR- and RRa-P3HT, the experimental spectra are broadened and red-shifted compared with the undoped polymers. The calculated IR spectra of polaron and bipolaron agree well with the trend of the experimental IR spectra of doped RR- and RRa-P3HT.

DOI: 10.1021/acs.jpcc.5b11764
J. Phys. Chem. C 2016, 120, 1994−2001

Table 1. Main Experimental IR, Raman, and PIA Vibrational Modes of RR- and RRa-P3HT, Calculated Electronic States, and Their Assignments

	mode wavenumber - experiment (cm^{-1})			mode wavenumber - theory (cm^{-1})					
polymer type (RR-, RRa-)	photodoping	IR	Raman	IR - ground	IR - polaron	IR - excited (singlet)	Raman - ground	mode assignment	optical activity
RR			599					C_α–S–C_α ring deformation	Raman
RR	681		678	686	689	680	696	C_α–S–C_α symmetric deformation	Raman
RRa	687			684	687	677			
RR	727	725	727	705				hexyl rocking vibration C_α–S–C_α antisymmetric deformation	IR Raman
RRa	731	727		712	708	697			
RR	818	820		814		813		C_β–H out-of-plane vibration C_α–S symmetric stretching	IR
RRa	820	827		812		811			
RR	1216				1191			C_β–H bending	IR
RRa	1218				1196				
RR	1324				1326			C_α=C_α symmetric stretching	IR
RRa	1326				1334				
RR	1386				1376			C_α–C_β symmetric stretching	IR
RRa	1388				1378				
RR	1375	1369	1382	1386		1354	1349	terminal CH_3 C_β–C_β symmetric stretching	IR Raman
RRa	1375	1373	1375	1387		1363			
RR	1450	1464	1450	1426		1446	1430	C_α=C_β symmetric stretching	IR, Raman IRAV
RRa	1458	1450, 1470	1458	1442		1448	1444		
RR	1512	1512	1512	1499		1486	1448	C_α=C_β antisymmetric stretching	IR, Raman IRAV
RRa	1522	1516	1522	1510		1500	1483		

When polarons or bipolarons are formed, the thiophene ring in the polymer repeat unit assumes a quinoid-like structure, with characteristic vibrational signatures in the region of 1200−1400 cm^{-1}. Specifically, the bands around 1324 cm^{-1} (RR) and 1326 cm^{-1} (RRa) (calc.: 1326 and 1334 cm^{-1}) are due to C_α=C_α bonds stretching between neighboring thiophene rings. Other bands at 1386 cm^{-1} (RR) and 1388 cm^{-1} (RRa) (calc.: 1376 and 1378 cm^{-1}) are ascribed to the inter-ring C_α–C_β symmetric stretching. The experimental IR transmittance band at 1216 cm^{-1} (RR) and 1218 cm^{-1} (RRa) (calc.: 1191 and 1196 cm^{-1}), assigned to C_β–H bending vibrations in the thiophene ring, becomes stronger compared with the same mode in the ground state (1201 and 1203 cm^{-1}).

Figure 3 also reports the theoretical Raman spectra of doped P3HT. In this case, the slight red shift of the experimental resonant Raman spectra compared with the calculated data may be due to a more equalized bond-length pattern than the one predicted.[60] Three main Raman bands for the doped samples at 1380, 1448, and 1510 cm^{-1} for RR-P3HT and at 1377, 1460, and 1517 cm^{-1} for RRa-P3HT, similar to those of undoped P3HT, arise from the C−C/C=C stretching modes delocalized over the entire oligomer. The calculated (non-resonant) Raman spectra of charged states of P3HT also show two main peaks at 1432 (RR) and 1412 cm^{-1} (RRa) for polarons and at 1372 (RR) and 1338 cm^{-1} (RRa) for bipolarons; however, the computed spectra are more structured than the experimental ones, and this may be due to the fact that calculations do not include resonance effects, which may enhance the peak intensity of some Raman-active modes.[7,61] Because C_α=C_α and C_β=C_β modes coexist in the quinoid structure of the doped polymer, some of the normal Raman modes can be attributed to totally symmetric stretching of C_α=C_α bonds, as previously reported by Casado et al. for doped oligothiophenes.[62] Overall, the comparative analysis of IR and Raman spectra of chemical doped-P3HT clearly indicates the transition from benzenoid to quinoid structure due to polaron or bipolaron formation.

Figure 4 shows the comparison between experimental photoinduced absorption, chemically induced absorption, and Raman spectra of RR- and RRa-P3HT in the 500−1700 cm^{-1} spectral region and the computed polaron, singlet-excited, and ground state IR modes. In both cases the PIA spectra were obtain exciting at 532 nm, close to the maximum of absorption of the two polymers (see Figure S2). Table 1 summarizes the main modes and their assignment. The IRAV modes of both samples can be attributed, on the basis of DFT and TD-DFT calculations, to peaks present in the IR spectra of polaron ($P3HT^+$), bipolaron ($P3HT^{+2}$), or excited state ($^1P3HT^*$) species and Raman spectra of the neutral species. RR- and RRa-P3HT show five principal negative photoinduced absorption (PIA) bands around 730, 800, 1360, 1450, and 1510 cm^{-1}. In the following we will focus our discussion on the differences induced by conformational disorder in *conventional* IRAV modes (i.e., those corresponding to Raman modes) in RR- and RRa-P3HT and on the origin of the mode around 800 cm^{-1}, which does not have a Raman counterpart.

The *conventional* IRAV modes, that is, 730, 1360, 1450, and 1510 cm^{-1}, can be associated with the active Raman modes of antisymmetric C_α–S–C_α deformation (727 and 731 cm^{-1} for RR and Ra, respectively), symmetric C_β–C_β stretching (1382 and 1375 cm^{-1} for RR and Ra, respectively), symmetric C_α=C_β stretching (1450 and 1458 cm^{-1} for RR and Ra, respectively), and antisymmetric C_α=C_β stretching (1512 and 1522 cm^{-1} for RR and Ra, respectively) vibrations of ground-state P3HT. PIA spectra of RR- and RRa-P3HT show significant differences in the 1300−1600 cm^{-1} region, specifically: (i) different intensity ratio between the ∼1450 and the ∼1360 cm^{-1} bands: $I_{1450/1360}$ (RRa-) < $I_{1450/1360}$ (RR-) and (ii) ∼1450 cm^{-1} band splitting in the case of RRa-P3HT—this is a direct consequence of the reduction of intensity and splitting of the 1443 cm^{-1} C=C stretching Raman mode

DOI: 10.1021/acs.jpcc.5b11764
J. Phys. Chem. C 2016, 120, 1994−2001

previously discussed for RRa-P3HT in the ground state. The PIA band of RR-P3HT around 1360 cm^{-1} can be interpreted as a superposition of the calculated IR spectra for polaron, bipolaron, and excited-state species. In this region are collocated the quinoid $C_\beta{=}C_\beta$ symmetric bond stretching modes at 1324 (polaron), 1325 (bipolaron), and 1330−1400 (excited state) cm^{-1} and the interring $C_\alpha{=}C_\alpha$ antisymmetric bonds stretching at 1384 (polaron), 1385 (bipolaron), and 1401 (excited state) cm^{-1}. Thus, the activity of these modes in the PIA spectra cannot be uniquely attributed to the IR and Raman spectra computed for the neutral species, rather to a *photoexcited* structure resembling that of exciton or polaronic species. In the case of RRa-P3HT, the 1360 cm^{-1} PIA band is also well reproduced by the computed IR spectra of polaron, bipolaron, and excited states, but it is more intense than in RR-P3HT. Thus, a thorough comparison between the PIA spectra and first-principles calculations can provide fine details of the degree of disorder of the polymeric chains.

The intense and specific PIA mode around 800 cm^{-1} cannot be ascribed to Raman mode conversion induced by charged excitations. This IR-active mode is due to the C_α−S stretching of the thiophene rings in the singlet excited state, whereas in the ground state normal modes in this spectral region are assigned to C_β−H out-of-plane deformation.[63,64]. Because this IR-active band has a large cross section in the excited state, the corresponding IRAV mode can be regarded as a signature of long-lived photoexcited excitonic species (^{1}P3HT*). Similar to carbon−carbon stretching modes, the intramolecular C_α−S stretching mode is very sensitive to the local chain conformations/distortions. Thus, the intensity ratio I_{817}/I_{730}, can be used as a spectroscopic marker of the polymer chain structure. Indeed, this ratio decreases from RR- to RRa-P3HT because of their different local intra- and interchain structure. To the authors' knowledge, this is the first observation of a vibrational signature of singlet excited states in the PIA spectra of P3HT, which provides a new probe for structural deformations induced by photoexcitations.

The two points discussed are crucial to draw proper structural-functional relationships of general validity for polymeric chains. RRa- chains are characterized by a larger ground-state structural distortion than RR-, leading to higher relaxations and favoring self-localization and charge trapping processes after the photoexcitation. Exciton, polaron, and bipolaron are generated on different time scales (from fs to ns), leading to localization processes and structural relaxation[65,66] with spectroscopic signatures sensitive to the local molecular conformations and order. Therefore, as results from our IRAV analysis, RRa- chains trap charges and localized the excitations more efficiently than RR-chains, leading to more structured IRAV spectral pattern (e.g., see intensity ratios 1450/1360 and 817/730 cm^{-1} bands, Figure 4).

In conclusion, by combining IR, Raman, and PIA-IR spectroscopy and quantum-chemical calculations, the signatures of polaron, bipolaron, and singlet excited states have been identified for both RR- and RRa-P3HT and correlated with the local molecular structure of the polymer. RRa-P3HT show higher structural relaxations and reorganizations upon excitations than RR-P3HT chains, leading to specific IRAV fingerprints (band splitting and intensity patterns) due to their different regioregularity. The proposed framework, beyond classical models, can be applied to a vast set of organic semiconductors to elucidate the chemical-physical mechanisms occurring upon photoexcitation (e.g., direct polaron generation and/or exciton localization and diffusion)[67] and to anticipate the extent of charge/exciton delocalization of newly synthesized materials with various degrees of disorder.

EXPERIMENTAL METHODS

Infrared absorption spectra were obtained in a Fourier transform infrared (FTIR) spectrometer (Bruker Vertex 80v) equipped with room-temperature DTGS detector. Spectral and phase resolution used during Fourier transformation were 4 and 32 cm^{-1}, respectively. Photo-induced absorption (PIA) spectra were recorded at low temperature (T = 78 K) by photoexciting the samples with at continuous wave green laser (λ_{ex} = 532 nm) and probing the induced change in transmission ($-\Delta T/T$) by an FTIR spectrometer equipped with an MCT detector. Thick (~3 μm) RR-P3HT and RRa-P3HT films were drop-cast on CaF_2 substrates for IR-PIA measurements in transmission-mode measurements in near-normal back scattering geometry. The differential signal of over 5000 consecutive scans with pump light on and off was averaged to increase the signal-to-noise ratio. Raman spectra were obtained in a Renishaw Raman microscope configured with a charge-coupled device array detector. A green (λ_{ex} = 532 nm) laser line was used for excitation with power below 1 mW. Raman signals were collected by a Leica 1003 objective lens (NA = 50.85) and dispersed by 2400 line/mm gratings with frequency resolution of 0.8 cm^{-1}. The integration time was 20 s.

ASSOCIATED CONTENT

Supporting Information

The Supporting Information is available free of charge on the ACS Publications website at DOI: 10.1021/acs.jpcc.5b11764.

Optimized molecular structures ground, polaron, bipolaron, and singlet excited states of RR- and RRa-P3HT, experimental absorption and photoluminescence spectra, calculated Raman spectra of RR-P3HT featuring different oligomer lengths, and vibrational normal modes for each. (PDF)

AUTHOR INFORMATION

Corresponding Authors

*D.F.: E-mail: fazzi@mpi-muelheim.mpg.de.

*C.S.: E-mail: csoci@ntu.edu.sg.

Notes

The authors declare no competing financial interest.

ACKNOWLEDGMENTS

Research was supported by the Singapore Ministry of Education (grant number MOE2013-T2-1-044) and the Singapore-Berkeley Research Initiative for Sustainable Energy (SinBeRISE) Create Programme. D.F. acknowledges the Alexander von Humboldt foundation for a Post Doctoral fellowship.

REFERENCES

(1) Venkateshvaran, D.; Nikolka, M.; Sadhanala, A.; Lemaur, V.; Zelazny, M.; Kepa, M.; Hurhangee, M.; Kronemeijer, A. J.; Pecunia, V.; Nasrallah, I.; et al. Approaching Disorder-Free Transport in High-Mobility Conjugated Polymers. *Nature* **2014**, *515*, 384−388.

(2) Li, G.; Zhu, R.; Yang, Y. Polymer Solar Cells. *Nat. Photonics* **2012**, *6*, 153−161.

DOI: 10.1021/acs.jpcc.5b11764
J. Phys. Chem. C 2016, 120, 1994−2001

(3) Castiglioni, C.; Tommasini, M.; Zerbi, G. Raman Spectroscopy of Polyconjugated Molecules and Materials: Confinement Effect in One and Two Dimensions. *Philos. Trans. R. Soc., A* **2004**, *362*, 2425−2459.
(4) DeLongchamp, D. M.; Kline, R. J.; Fischer, D. A.; Richter, L. J.; Toney, M. F. Molecular Characterization of Organic Electronic Films. *Adv. Mater.* **2011**, *23*, 319−337.
(5) Kang, I.; Yun, H. J.; Chung, D. S.; Kwon, S. K.; Kim, Y. H. Record High Hole Mobility in Polymer Semiconductors Via Side-Chain Engineering. *J. Am. Chem. Soc.* **2013**, *135*, 14896−14899.
(6) Castiglioni, C.; Delzoppo, M.; Zerbi, G. Vibrational Raman-Spectroscopy of Polyconjugated Organic Oligomers and Polymers. *J. Raman Spectrosc.* **1993**, *24*, 485−494.
(7) Negri, F.; di Donato, E.; Tommasini, M.; Castiglioni, C.; Zerbi, G.; Mullen, K. Resonance Raman Contribution to the D Band of Carbon Materials: Modeling Defects with Quantum Chemistry. *J. Chem. Phys.* **2004**, *120*, 11889−11900.
(8) Hernandez, V.; Casado, J.; Ramirez, F. J.; Zotti, G.; Hotta, S.; Navarrete, J. T. L. Efficient Pi Electrons Delocalization in Alpha,Alpha'-Dimethyl End-Capped Oligothiophenes: A Vibrational Spectroscopic Study. *J. Chem. Phys.* **1996**, *104*, 9271−9282.
(9) Hernandez, V.; Castiglioni, C.; Delzoppo, M.; Zerbi, G. Confinement Potential and Pi-Electron Delocalization in Polyconjugated Organic Materials. *Phys. Rev. B: Condens. Matter Mater. Phys.* **1994**, *50*, 9815−9823.
(10) Casado, J.; Ortiz, R. P.; Navarrete, J. T. L. Quinoidal Oligothiophenes: New Properties Behind an Unconventional Electronic Structure. *Chem. Soc. Rev.* **2012**, *41*, 5672−5686.
(11) Fazzi, D.; Caironi, M. Multi-Length-Scale Relationships between the Polymer Molecular Structure and Charge Transport: The Case of Poly-Naphthalene Diimide Bithiophene. *Phys. Chem. Chem. Phys.* **2015**, *17*, 8573−8590.
(12) Hwang, I.; Scholes, G. D. Electronic Energy Transfer and Quantum-Coherence in Pi-Conjugated Polymers. *Chem. Mater.* **2011**, *23*, 610−620.
(13) Banerji, N. Sub-Picosecond Delocalization in the Excited State of Conjugated Homopolymers and Donor-Acceptor Copolymers. *J. Mater. Chem. C* **2013**, *1*, 3052−3066.
(14) Di Nuzzo, D.; Fontanesi, C.; Jones, R.; Allard, S.; Dumsch, I.; Scherf, U.; von Hauff, E.; Schumacher, S.; Da Como, E. How Intermolecular Geometrical Disorder Affects the Molecular Doping of Donor-Acceptor Copolymers. *Nat. Commun.* **2015**, *6*, 6460.
(15) Wang, C.; Angelella, M.; Doyle, S. J.; Lytwak, L. A.; Rossky, P. J.; Holliday, B. J.; Tauber, M. J. Resonance Raman Spectroscopy of the T1 Triplet Excited State of Oligothiophenes. *J. Phys. Chem. Lett.* **2015**, *6*, 3521−3527.
(16) Diesinger, H.; Chan, E. A.; Yin, J.; Soci, C. Ultrafast Charge Carrier Dynamics in Organic (Opto)Electronic Materials. In *Handbook of Organic Materials for Optical and Optoelectronic Devices: Properties and Applications*; Ostroverkhova, O., Ed.; Woodhead Publishing Series in Electronic and Optical Materials: 2013.
(17) Wilson, E. B.; Decius, J. C.; Cross, P. C. *Molecular Vibrations: The Theory of Infrared and Raman Vibrational Spectra*; Dover Books on Chemistry: 2001
(18) Cross, P. C.; Wilson, E. B.; Decius, J. C.. *Molecular Vibrations: The Theory of Infrared and Raman Vibrational Spectra*; Dover Books on Chemistry: 1980.
(19) Lucotti, A.; Tommasini, M.; Fazzi, D.; Del Zoppo, M.; Chalifoux, W. A.; Ferguson, M. J.; Zerbi, G.; Tykwinski, R. R. Evidence for Solution-State Nonlinearity of Sp-Carbon Chains Based on Ir and Raman Spectroscopy: Violation of Mutual Exclusion. *J. Am. Chem. Soc.* **2009**, *131*, 4239−4244.
(20) Milani, A.; Tommasini, M.; Del Zoppo, M.; Castiglioni, C.; Zerbi, G. Carbon Nanowires: Phonon and Pi-Electron Confinement. *Phys. Rev. B: Condens. Matter Mater. Phys.* **2006**, *74*, 153418.
(21) Bredas, J. L.; Street, G. B. Polarons, Bipolarons, and Solitons in Conducting Polymers. *Acc. Chem. Res.* **1985**, *18*, 309−315.
(22) Heeger, A. J.; Sariciftci, N. S.; Namdas, E. B. *Semiconducting and Metallic Polymers*; Oxford University Press: New York, 2010.
(23) Soci, C.; Moses, D.; Xu, Q. H.; Heeger, A. J. Charge-Carrier Relaxation Dynamics in Highly Ordered Poly(P-Phenylene Vinylene): Effects of Carrier Bimolecular Recombination and Trapping. *Phys. Rev. B: Condens. Matter Mater. Phys.* **2005**, *72*, 245204.
(24) Galimberti, D.; Milani, A.; Castiglioni, C. Infrared Intensities and Charge Mobility in Hydrogen Bonded Complexes. *J. Chem. Phys.* **2013**, *139*, 074304.
(25) Pensack, R. D.; Asbury, J. B. Beyond the Adiabatic Limit: Charge Photogeneration in Organic Photovoltaic Materials. *J. Phys. Chem. Lett.* **2010**, *1*, 2255−2263.
(26) Osterbacka, R.; An, C. P.; Jiang, X. M.; Vardeny, Z. V. Two-Dimensional Electronic Excitations in Self-Assembled Conjugated Polymer Nanocrystals. *Science* **2000**, *287*, 839−842.
(27) Li, Z. Q.; Wang, G. M.; Sai, N.; Moses, D.; Martin, M. C.; Di Ventra, M.; Heeger, A. J.; Basov, D. N. Infrared Imaging of the Nanometer-Thick Accumulation Layer in Organic Field-Effect Transistors. *Nano Lett.* **2006**, *6*, 224−228.
(28) Kim, Y. H.; Spiegel, D.; Hotta, S.; Heeger, A. J. Photoexcitation and Doping Studies of Poly(3-Hexylthienylene). *Phys. Rev. B: Condens. Matter Mater. Phys.* **1988**, *38*, 5490−5495.
(29) Fincher, C. R., Jr.; Ozaki, M.; Heeger, A. J.; MacDiarmid, A. G. Donor and Acceptor States in Lightly Doped Polyacetylene, (Ch)_{X}. *Phys. Rev. B: Condens. Matter Mater. Phys.* **1979**, *19*, 4140−4148.
(30) Schaffer, H. E.; Friend, R. H.; Heeger, A. J. Localized Phonons Associated with Solitons in Polyacetylene - Coupling to the Nonuniform Mode. *Phys. Rev. B: Condens. Matter Mater. Phys.* **1987**, *36*, 7537−7541.
(31) Miranda, P. B.; Moses, D.; Heeger, A. J. Ultrafast Photogeneration of Charged Polarons in Conjugated Polymers. *Phys. Rev. B: Condens. Matter Mater. Phys.* **2001**, *64*, 081201.
(32) Osterbacka, R.; Jiang, X. M.; An, C. P.; Horovitz, B.; Vardeny, Z. V. Photoinduced Quantum Interference Antiresonances in Pi-Conjugated Polymers. *Phys. Rev. Lett.* **2002**, *88*, 226401.
(33) Lee, K. H.; Janssen, R. A. J.; Sariciftci, N. S.; Heeger, A. J. Direct Evidence of Photoinduced Electron-Transfer in Conducting-Polymer-C60 Composites by Infrared Photoexcitation Spectroscopy. *Phys. Rev. B: Condens. Matter Mater. Phys.* **1994**, *49*, 5781−5784.
(34) Sheng, C. X.; Basel, T.; Pandit, B.; Vardeny, Z. V. Photoexcitation Dynamics in Polythiophene/Fullerene Blends for Photovoltaic Applications. *Org. Electron.* **2012**, *13*, 1031−1037.
(35) Jiang, X. M.; Osterbacka, R.; Korovyanko, O.; An, C. P.; Horovitz, B.; Janssen, R. A. J.; Vardeny, Z. V. Spectroscopic Studies of Photoexcitations in Regioregular and Regiorandom Polythiophene Films. *Adv. Funct. Mater.* **2002**, *12*, 587−597.
(36) Jiang, X. M.; An, C. P.; Osterbacka, R.; Vardeny, Z. V. Ftir Studies of Charged Photoexcitations in Regio-Regular and Regio-Random Poly(3-Alkylthiophene) Films. *Synth. Met.* **2001**, *116*, 203−206.
(37) Chin, X. Y.; Yin, J.; Wang, Z.; Caironi, M.; Soci, C. Mapping Polarons in Polymer Fets by Charge Modulation Microscopy in the Mid-Infrared. *Sci. Rep.* **2014**, *4*, 3626.
(38) Khatib, O.; Mueller, A. S.; Stinson, H. T.; Yuen, J. D.; Heeger, A. J.; Basov, D. N. Electron and Hole Polaron Accumulation in Low-Bandgap Ambipolar Donor-Acceptor Polymer Transistors Imaged by Infrared Microscopy. *Phys. Rev. B: Condens. Matter Mater. Phys.* **2014**, *90*, 235307.
(39) Wang, Z. L.; Zhao, J.; Frank, B.; Ran, Q. D.; Adamo, G.; Giessen, H.; Soci, C. Plasmon-Polaron Coupling in Conjugated Polymer on Infrared Nanoantennas. *Nano Lett.* **2015**, *15*, 5382−5387.
(40) Horovitz, B. Infrared Activity of Peierls Systems and Application to Polyacetylene. *Solid State Commun.* **1982**, *41*, 729−734.
(41) Horovitz, B.; Gutfreund, H.; Weger, M. Infrared and Raman Activities of Organic Linear Conductors. *Phys. Rev. B: Condens. Matter Mater. Phys.* **1978**, *17*, 2796−2799.
(42) Zerbi, G.; Castiglioni, C. *Conjugated Polymers*; Kluwer Academic Publishers: 1991.
(43) Horovitz, B.; Osterbacka, R.; Vardeny, Z. V. Multiple Fano Effect in Charge Density Wave Systems. *Synth. Met.* **2004**, *141*, 179−183.

DOI: 10.1021/acs.jpcc.5b11764
J. Phys. Chem. C 2016, 120, 1994−2001

(44) Yildizhan, M. M.; Fazzi, D.; Milani, A.; Brambilla, L.; Del Zoppo, M.; Chalifoux, W. A.; Tykwinski, R. R.; Zerbi, G. Photogenerated Cumulenic Structure of Adamantyl Endcapped Linear Carbon Chains: An Experimental and Computational Investigation Based on Infrared Spectroscopy. *J. Chem. Phys.* **2011**, *134*, 124512.
(45) Fazzi, D.; Scotognella, F.; Milani, A.; Brida, D.; Manzoni, C.; Cinquanta, E.; Devetta, M.; Ravagnan, L.; Milani, P.; Cataldo, F.; et al. Ultrafast Spectroscopy of Linear Carbon Chains: The Case of Dinaphthylpolyynes. *Phys. Chem. Chem. Phys.* **2013**, *15*, 9384−9391.
(46) Gierschner, J.; Cornil, J.; Egelhaaf, H. J. Optical Bandgaps of Pi-Conjugated Organic Materials at the Polymer Limit: Experiment and Theory. *Adv. Mater.* **2007**, *19*, 173−191.
(47) Frisch, M. J.; Trucks, G. W.; Schlegel, H. B.; Scuseria, G. E.; Robb, M. A.; Cheeseman, J. R.; Scalmani, G.; Barone, V.; Mennucci, B.; Petersson, G. A.; et al. *Gaussian 09*; Gaussian, Inc.: Wallingford, CT, 2009.
(48) Casado, J.; Zgierski, M. Z.; Ewbank, P. C.; Burand, M. W.; Janzen, D. E.; Mann, K. R.; Pappenfus, T. M.; Berlin, A.; Perez-Inestrosa, E.; Ortiz, R. P.; et al. Exploration of Ground and Excited Electronic States of Aromatic and Quinoid S,S-Dioxide Terthiophenes. Complementary Systems for Enhanced Electronic Organic Materials. *J. Am. Chem. Soc.* **2006**, *128*, 10134−10144.
(49) Casado, J.; Hernandez, V.; Ortiz, R. P.; Delgado, M. C. R.; Navarrete, J. T. L.; Fuhrmann, G.; Bauerle, P. Application of Raman Spectroscopy and Quantum Chemistry for Featuring the Structure of Positively Charged Species in Macrocyclic Pi-Conjugated Diacetylene-Bridged Oligothiophenes. *J. Raman Spectrosc.* **2004**, *35*, 592−599.
(50) Salzner, U.; Aydin, A. Improved Prediction of Properties of Pi-Conjugated Oligomers with Range-Separated Hybrid Density Functionals. *J. Chem. Theory Comput.* **2011**, *7*, 2568−2583.
(51) Fazzi, D.; Caironi, M.; Castiglioni, C. Quantum-Chemical Insights into the Prediction of Charge Transport Parameters for a Naphthalenetetracarboxydiimide-Based Copolymer with Enhanced Electron Mobility. *J. Am. Chem. Soc.* **2011**, *133*, 19056−19059.
(52) Kronik, L.; Stein, T.; Refaely-Abramson, S.; Baer, R. Excitation Gaps of Finite-Sized Systems from Optimally Tuned Range-Separated Hybrid Functionals. *J. Chem. Theory Comput.* **2012**, *8*, 1515−1531.
(53) Casado, J.; Hernandez, V.; Kanemitsu, Y.; Navarrete, J. T. L. Infrared and Raman Spectra of a New Radical Cation Charged Defect Created on a Well-Barrier-Well Thiophene-Based Oligomer. *J. Raman Spectrosc.* **2000**, *31*, 565−570.
(54) Malagoli, M.; Coropceanu, V.; da Silva Filho, D. A.; Bredas, J. L. A Multimode Analysis of the Gas-Phase Photoelectron Spectra in Oligoacenes. *J. Chem. Phys.* **2004**, *120*, 7490−7496.
(55) Irikura, K. K.; Johnson, R. D.; Kacker, R. N. Uncertainties in Scaling Factors for Ab Initio Vibrational Frequencies. *J. Phys. Chem. A* **2005**, *109*, 8430−8437.
(56) Brambilla, L.; Tommasini, M.; Botiz, I.; Rahimi, K.; Agumba, J. O.; Stingelin, N.; Zerbi, G. Regio-Regular Oligo and Poly(3-Hexyl Thiophene): Precise Structural Markers from the Vibrational Spectra of Oligomer Single Crystals. *Macromolecules* **2014**, *47*, 6730−6739.
(57) Tsoi, W. C.; James, D. T.; Kim, J. S.; Nicholson, P. G.; Murphy, C. E.; Bradley, D. D. C.; Nelson, J.; Kim, J. S. The Nature of in-Plane Skeleton Raman Modes of P3HT and Their Correlation to the Degree of Molecular Order in P3HT:PCBM Blend Thin Films. *J. Am. Chem. Soc.* **2011**, *133*, 9834−9843.
(58) Fei, Z. P.; Boufflet, P.; Wood, S.; Wade, J.; Moriarty, J.; Gann, E.; Ratcliff, E. L.; McNeill, C. R.; Sirringhaus, H.; Kim, J. S.; et al. Influence of Backbone Fluorination in Regioregular Poly(3-Alkyl-4-Fluoro)Thiophenes. *J. Am. Chem. Soc.* **2015**, *137*, 6866−6879.
(59) Casado, J.; Hernandez, V.; Delgado, M. C. R.; Ortiz, R. P.; Navarrete, J. T. L.; Facchetti, A.; Marks, T. J. Incisive Structure-Spectroscopic Correlation in Oligothiophenes Functionalized with (±) Inductive/Mesomeric Fluorine Groups: Joint Raman and Dft Study. *J. Am. Chem. Soc.* **2005**, *127*, 13364−13372.
(60) Singh, R. K.; Kumar, J.; Singh, R.; Kant, R.; Rastogi, R. C.; Chand, S.; Kumar, V. Structure-Conductivity Correlation in Ferric Chloride-Doped Poly(3-hexylthiophene). *New J. Phys.* **2006**, *8*, 112.
(61) Neugebauer, J.; Hess, B. A. Resonance Raman Spectra of Uracil Based on Kramers-Kronig Relations Using Time-Dependent Density Functional Calculations and Multireference Perturbation Theory. *J. Chem. Phys.* **2004**, *120*, 11564−11577.
(62) Casado, J.; Katz, H. E.; Hernandez, V.; Lopez Navarrete, J. T.; Navarrete, J. T. Spectroelectrochemical Raman Study of Two End-Capped Sexithiophenes with Applications as Electroactive Molecular Materials. *J. Phys. Chem. B* **2002**, *106*, 2488−2496.
(63) Giussani, E.; Fazzi, D.; Brambilla, L.; Caironi, M.; Castiglioni, C. Molecular Level Investigation of the Film Structure of a High Electron Mobility Copolymer Via Vibrational Spectroscopy. *Macromolecules* **2013**, *46*, 2658−2670.
(64) Giussani, E.; Brambilla, L.; Fazzi, D.; Sommer, M.; Kayunkid, N.; Brinkmann, M.; Castiglioni, C. Structural Characterization of Highly Oriented Naphthalene-Diimide-Bithiophene Copolymer Films Via Vibrational Spectroscopy. *J. Phys. Chem. B* **2015**, *119*, 2062−2073.
(65) Magyar, R. J.; Tretiak, S. Dependence of Spurious Charge-Transfer Excited States on Orbital Exchange in Tddft: Large Molecules and Clusters. *J. Chem. Theory Comput.* **2007**, *3*, 976−987.
(66) Fazzi, D.; Barbatti, M.; Thiel, W. Modeling Ultrafast Exciton Deactivation in Oligothiophenes Via Nonadiabatic Dynamics. *Phys. Chem. Chem. Phys.* **2015**, *17*, 7787−7799.
(67) Song, Y.; Hellmann, C.; Stingelin, N.; Scholes, G. D. The Separation of Vibrational Coherence from Ground- and Excited-Electronic States in P3HT Film. *J. Chem. Phys.* **2015**, *142*, 212410.

DOI: 10.1021/acs.jpcc.5b11764
J. Phys. Chem. C 2016, 120, 1994−2001